

# Droplet and Aerosol Generation With Mastoidectomy During the COVID-19 Pandemic: Assessment of Baseline Risk and Mitigation Measures With a High-performance Cascade Impactor

\*Monika E. Freiser, \*Harish Dharmarajan, †Devi Sai Sri Kavya Boorgu, †Edward S. Sim, ‡Timothy E. Corcoran, \*§Noel Jabbour, and \*§David H. Chi

\*Department of Otolaryngology, University of Pittsburgh Medical Center; †University of Pittsburgh School of Medicine, University of Pittsburgh; ‡Division of Pulmonary, Allergy, and Critical Care Medicine; and §Children's Hospital of Pittsburgh, Pittsburgh, PA

---

**Hypothesis:** Aerosols are generated during mastoidectomy and mitigation strategies may effectively reduce aerosol spread.

**Background:** An objective understanding of aerosol generation and the effectiveness of mitigation strategies can inform interventions to reduce aerosol risk from mastoidectomy and other open surgeries involving drilling.

**Methods:** Cadaveric and fluorescent three-dimensional printed temporal bone models were drilled under variable conditions and mitigation methods. Aerosol production was measured with a cascade impactor set to detect particle sizes under 14.1  $\mu\text{m}$ . Field contamination was determined with examination under UV light.

**Results:** Drilling of cadaveric bones and three-dimensional models resulted in strongly positive aerosol production, measuring positive in all eight impactor stages for the

cadaver trials. This occurred regardless of using coarse or cutting burs, irrigation, a handheld suction, or an additional parked suction. The only mitigation factor that led to a completely negative aerosol result in all eight stages was placing an additional microscope drape to surround the field. Bone dust was scattered in all directions from the drill, including on the microscope, the surgeon, and visually suspended in the air for all but the drape trial.

**Conclusions:** Aerosols are generated with drilling the mastoid. Using an additional microscope drape to cover the surgical field was an effective mitigation strategy to prevent fine aerosol dispersion while drilling. **Key Words:** Aerosol—Coronavirus—COVID-19—Droplet—Mastoidectomy—Safety.

*Otol Neurotol* 42:614–622, 2021.

---

Understanding aerosol production during mastoid surgery and ways to mitigate aerosols and other debris may reduce the risk of SARS-CoV-2 coronavirus transmission. Mastoid and middle ear mucosa is in continuity with nasopharyngeal mucosa and may be a source of viral particles in an infected patient. Mastoidectomy has been categorized as an aerosol-generating procedure; however, there is limited data in the literature regarding the aerosol risk with mastoid drilling (1,2). Several studies have investigated the degree of debris scatter

when performing mastoidectomy (3,4), including one study that noted scatter as far as 6 feet (4). Chari et al. (5) recently investigated fine aerosol production using an optical particle size spectrometer placed at 30 cm and found significant particle production of aerosols in the sizes of 1 to 10  $\mu\text{m}$ . Norris et al. (6) in 2010 investigated the production of respirable particles during mastoidectomy using PVC filter cassettes set 50 cm from the field and found no detectible respirable particles; mastoidectomy did not meet requirements for respirator use. Given the limited data in the literature, there is a need to further elucidate the production of fine aerosols under 20  $\mu\text{m}$ , which are those most likely to remain airborne and be inhaled into the airway (7); aerosols with an aerodynamic diameter  $<5 \mu\text{m}$  can reach the alveoli and particles  $<10 \mu\text{m}$  can penetrate below the glottis. Additionally, particles between 10 and 20  $\mu\text{m}$  settle more readily and particles  $>20 \mu\text{m}$  have a ballistic trajectory (7). This study evaluates aerosol risk with mastoid drilling by utilizing a cascade impactor to collect fine aerosols of different aerodynamic sizes; particles are separated based on the principle of inertial impaction (8). Generated debris

---

Address correspondence and reprint requests to Harish Dharmarajan, M.D., Department of Otolaryngology, UPMC, Eye and Ear Institute, Suite 500, 200 Lothrop Street, Pittsburgh, PA 15213; E-mail: dharmarajan@upmc.edu

M.E.F. and H.D. are co-first authors, with equal contribution to the work.

There were no sources of funding for this project.

This project has not been presented or published in previous meetings.

The authors disclose no conflicts of interest.

Supplemental digital content is available in the text.

DOI: 10.1097/MAO.0000000000002987

particles with a smaller aerodynamic diameter have a lower tendency to be collected until the final impaction stages. To ensure that the collected aerosols originated from the specimen, Vitamin B2 was used as a fluorescent tracer in the irrigation, coating the entire mastoid drilling surface (9,10). The goals of this study were to objectively characterize whether aerosols of an aerodynamic diameter known to enter the airway are generated during mastoidectomy, map the field contamination of visible debris, and to test aerosol mitigation strategies.

## METHODS

### Preparation

This study was conducted with approval from the University of Pittsburgh Committee for Oversight of Research and Clinical Training Involving Decedents. A drilling station at a temporal bone laboratory was cleaned and prepared for use. The Anspach eMax2 drill (Johnson & Johnson, New Brunswick, NJ) was set for 80,000 revolutions per minute. Several suction ports were available for use during the trials at maximum wall suction capacity (150 mm Hg). A solution of 1 g/L vitamin B2 (riboflavin) in 0.9% normal saline was prepared as fluorescent irrigation. This was found to be a better marker for fine aerosols than fluorescein (10). For trials that included irrigation, the fluorescent irrigant was applied by an assistant via a squeeze bottle in a pulsatile fashion of about one pulse per second to keep the field appropriately moist. The total volume of irrigant may have varied between trials. For cadaveric trials, a formaldehyde preserved adult human cadaveric temporal bone was used. For three-dimensional (3D) model trials, two 3D temporal bone models were designed using an adult computed tomography scan and printed with the Formlabs 2 printer, via a previously described process (11). The material used was Formlabs white resin (Formlabs, Somerville, MA), which is inherently fluorescent. The 3D model trials were performed as an adjunct to the cadaveric trials to provide a highly visible, fluorescent medium to test. This would allow for detection of debris generated during mastoidectomy and provide a means to corroborate with the cadaveric and historic results. The material is not an exact replica of bone but does drill similarly as evaluated previously (11). Cortical mastoidectomy with extensive saucerization was performed for the trials. The amount of bone removed was not standardized; however, the time of each trial was set at 2 minutes. The start point was the stopping point of the previous trial, using a total one cadaveric bone and two 3D-printed models.

### Impactor Trials

A Model 170 Next Generation Impactor (NGI) was used to filter particles of the following eight aerodynamic diameter stages ( $D_{50}$ , cutoff diameter at 50% collection efficiency): 14.1  $\mu\text{m}$ , 8.61  $\mu\text{m}$ , 5.39  $\mu\text{m}$ , 3.30  $\mu\text{m}$ , 2.08  $\mu\text{m}$ , 1.36  $\mu\text{m}$ , 0.98  $\mu\text{m}$ , and less than 0.98  $\mu\text{m}$  (8). Each impactor stage reflects an average particle aerodynamic diameter given an input flow rate of 15 L per minute. With this particle size range, the impactor identifies aerosols that are most likely to settle in the lung, noted to occur most with particles under 5  $\mu\text{m}$  (12). The NGI input nozzle was placed 4 cm away from the edge of the cadaveric specimen or the 3D-printed temporal bone model, at a 45-degree angle above and to the right of the field (Fig. 1). This was the closest possible distance that allowed for space for instrumentation. This distance was selected to maximize the

chance of detecting any produced aerosols before being diluted by ambient air below the detection limit of the impactor. The impactor vacuum was suctioning in air at a rate of 15 L per minute for 2 minutes for each trial and continuously sampling while the surgeon was drilling. All particles suctioned in would travel through the collection ports and become trapped if they were of the designated aerodynamic diameters.

Following each trial, presence or absence of collected particles was visually assessed under direct visualization with UV illumination. An impactor stage was read as "positive" when material was seen trapped in a given stage's filter (Fig. 2). A baseline trial was performed before any mastoid drilling to measure the ambient room air. All eight stages were negative, indicating no detected aerosols for the measured sizes, when sampling room air. Between each trial, the aluminum foil pieces lining the collection chambers were replaced and the impactor was thoroughly cleaned to prevent cross-contamination between trials. Each trial was performed lasting 2 minutes each and one trial was performed for each condition.

The first trial was performed drilling cadaveric bone with a size 6 cutting bur, using B2 irrigation administered onto the field at one pulse per second, and one size 8 suction irrigator connected to suction only, finger occluded per discretion of the surgeon. The second trial involved use of a 4 diamond bur, B2 irrigation, and one size 8 handheld suction. In the third trial, we used a 6 cutting bur, B2 irrigation, one size 8 handheld suction and an additional patent suction tube parked adjacent to the specimen; this was to evaluate the effectiveness of an additional suction in the field for mitigating aerosol risk. A fourth trial consisted of using an additional microscope drape to cover the field. In this scenario, one drape was used to drape the microscope as is standard intraoperatively, but a second drape was secured with tape at the lens piece after removing just the lens cover, inverted, and draped over the surgical field (Supplemental Video, <http://links.lww.com/MAO/B144>). The surgeon operated from under the drape and the assistant applied irrigation through one of the eyepiece ports.

Trials performed on 3D printed models included two of those performed on cadaveric models as well as additional trials without irrigation and/or suction. The first trial was using a 6 cutting bur with no irrigation or suction. The second trial was using a 4 diamond bur with no irrigation or suction. The third trial was using a 6 cutting bur with an 8 handheld suction but no irrigation. The fourth trial was using a 6 cutting bur, one size 8 handheld suction, an additional adjacent parked suction, and no irrigation. The fifth trial was using a 6 cutting bur, B2 irrigation, and an 8 handheld suction.

### Field Contamination Trials

Field contamination trials were performed to visualize the production and spread of bone dust, irrigation droplets, and debris when drilling a fluorescent 3D temporal bone model. The 3D models were centered onto a black tarp which was labeled with 15 cm increment markers using orange tape. The personal protective equipment (PPE) of the surgeon included a surgical gown, gloves, and facemask. Both the tarp layout and each provider's PPE were checked with UV light to ensure no baseline debris or fluorescent contamination before the start of each trial. Each drilling scenario was conducted by a right-handed surgeon and performed for 2 minutes each. Trials were designed to test if the following variables affected the degree and pattern of field contamination on the tarp: drill bur type (6 cutting bur versus 4 diamond bur), use of Vitamin B2 irrigation (1 g/L solution in 0.9% normal saline), use of rigid suction (8 Fr), and use of an additional parked field suction (open suction

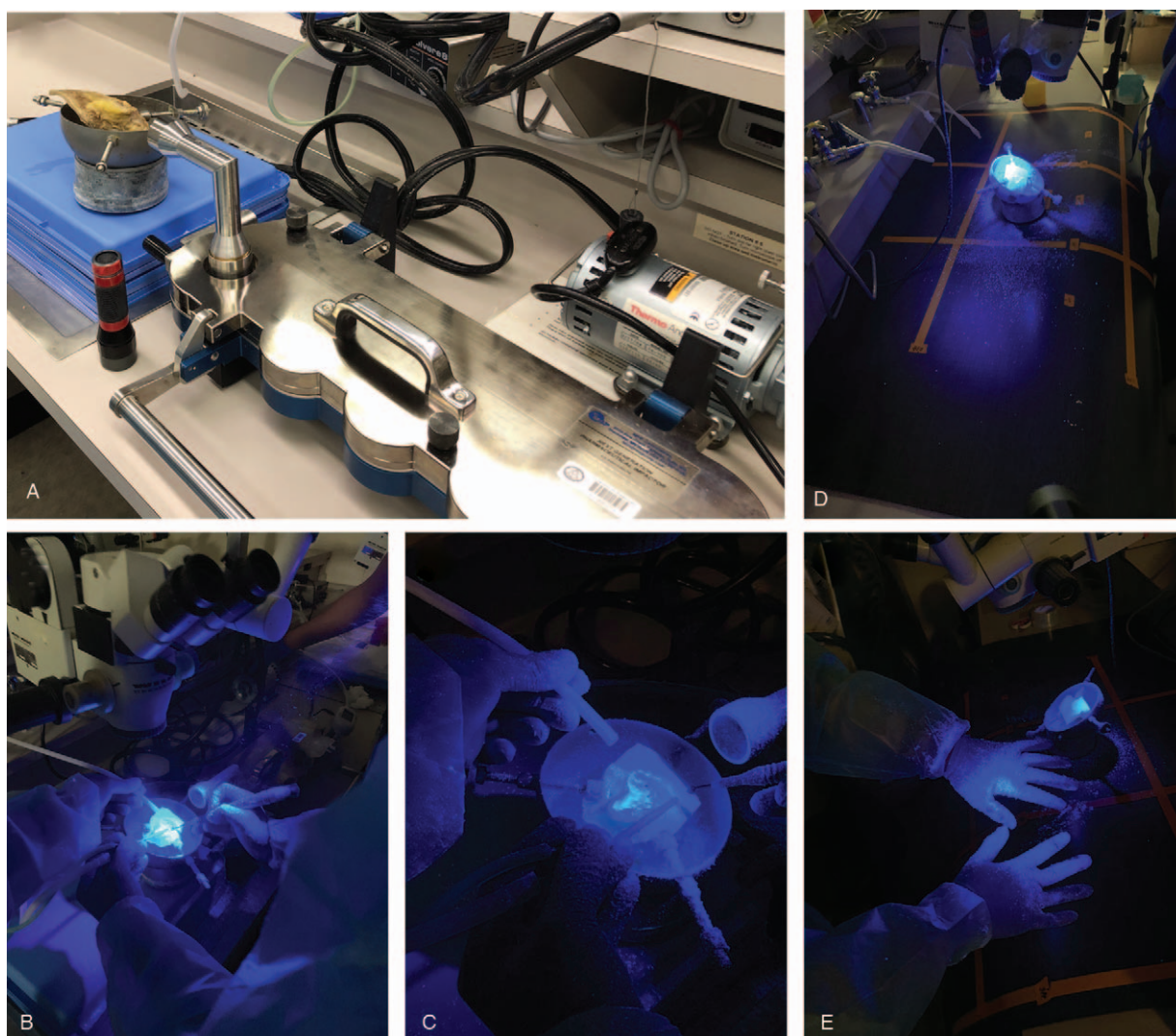


**FIG. 1.** Experimental setup for impactor trials and field contamination trials. A–C, Experimental setup of an impactor study with the impactor inlet positioned at the edge of the temporal bone holder during drilling. The pictured trial is the 3D-printed temporal bone with a 6 cutting bur, a handheld size 8 suction, and an additional parked field suction. D, E, The temporal bone holder is on the top of a tarp with 15 cm distances marked. After each 2-minute trial, the tarp is examined for debris. Note the amount of debris noted after the cortex was removed in the first 3D model 6 cutting bur trial.

tube adjacent to the specimen). After each 2-minute drilling trial, each 15 cm square of the tarp was visually examined using a UV light. The UV light was next shined on the provider's PPE and visual observations were noted. For each 15 cm quadrant on the tarp, a value of field contamination was assigned: 1) no perceptible particulate matter, 2) low (1–25%) field coverage, 3) intermediate (25–50%) field coverage, 4) major (50–75%) field coverage, and 5) heavy or excess field coverage (75–100%) with layer of dust caking.

## RESULTS

### Aerosol Impactor Survey

Drilling the cadaveric bone and the temporal bone models yielded notable aerosol production under  $14.1\ \mu\text{m}$  (Table 1). When drilling the cadaveric temporal bone with a 6 cutting bur, a size 8 handheld suction and B2 irrigation, all eight stages were strongly positive,

indicating aerosol production under  $14.1\ \mu\text{m}$ . All eight stages were also positive with the 4 diamond bur trial. When a 6 cutting bur, B2 irrigation, a size eight handheld suction and a parked suction tube adjacent to the drilling site were used, again all eight stages were positive (Fig. 2) Similarly, all trials drilling the 3D temporal bone model, which include cutting bur, diamond bur, handheld suction, and parked suction, were positive in stages 1 through 6, and positive in stages 1 through 7 when B2 irrigation was used. Ultimately, using irrigation, a parked suction, or changing the burr size during the trials did not eliminate aerosol production in either the cadaveric or 3D model trials. The only mitigation factor tested that led to complete elimination of detected aerosol was using a drape as a field barrier. When the microscope drape was used to cover the field, the impactor trial yielded negative findings across all stages showing lack of detectable fine

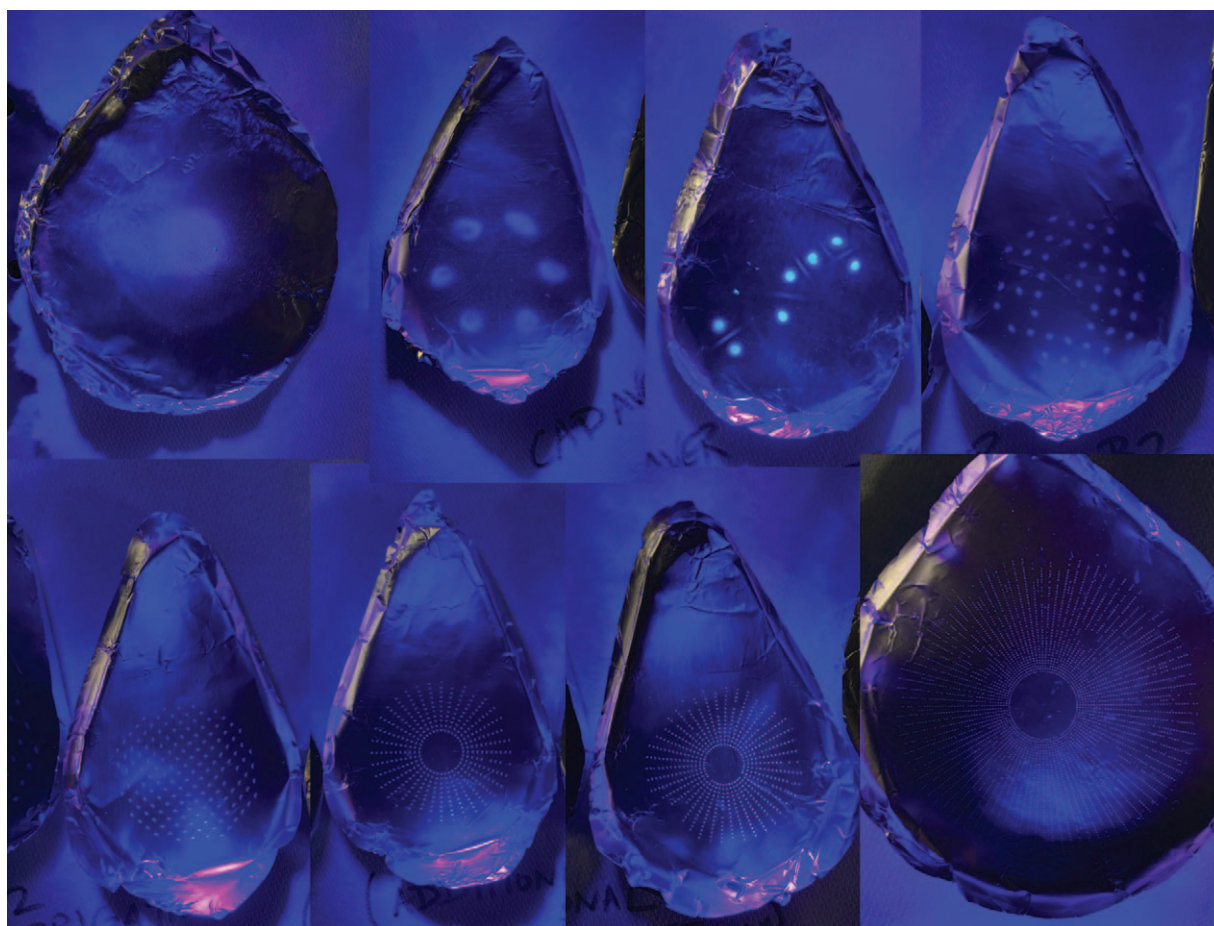


**FIG. 2.** Representative positive impactor trial result. All eight filters were positive in this trial, indicated by visible patterns in each filter. Aerosol size captured goes from 14  $\mu\text{m}$  in the upper left foil to 1  $\mu\text{m}$  on the bottom right foil. This trial was the cadaveric bone using a size 6 cutter bur, B2 irrigation, size 8 handheld suction, and parked patent suction tube adjacent to the mastoid cavity. A diffusely positive result was noted despite two suctions in the field.

**TABLE 1.** Impactor stage results for mastoid drilling under different scenarios using 3D-printed models and cadaveric temporal bone

Trial			Aerosol Particle Size ( $\mu\text{m}$ ) - D50 at 15 L/min							
Drill	Suction	Irrigation	14.1	8.61	5.39	3.30	2.08	1.36	0.98	<0.98
3D Printed Temporal Bone										
6 Cutter	N/A	N/A	+	+	+	+	+	+	-	-
4 Diamond	N/A	N/A	+	+	+	+	+	+	-	-
6 Cutter	8 Suction	N/A	+	+	+	+	+	+	-	-
6 Cutter	8 Suction Parked Suction	N/A	+	+	+	+	+	+	-	-
6 Cutter	8 Suction	B2	+	+	+	+	+	+	+	-
Cadaveric Temporal Bone										
6 Cutter	8 Suction	B2	+	+	+	+	+	+	+	+
6 Cutter	8 Suction Parked Suction	B2	+	+	+	+	+	+	+	+
6 Cutter	8 Suction	Saline	+	+	+	+	+	+	+	+
<sup>a</sup> 4 Diamond	8 Suction	B2	+	+	+	+	+	+	+	+
<sup>b</sup> 6 Cutter	8 Suction	B2	-	-	-	-	-	-	-	-

Aerosol particulate size following simulated mastoidectomy with 3D-printed temporal bone model and cadaveric temporal bone.

Visible aerosol particle matter for 3D-printed temporal bone model appeared blue colored under UV light.

<sup>a</sup>Cadaver model was soaked overnight in 1 g/L vitamin B2.

<sup>b</sup>Procedure was covered with a microscope drape, see Figure 5 for experimental setup.

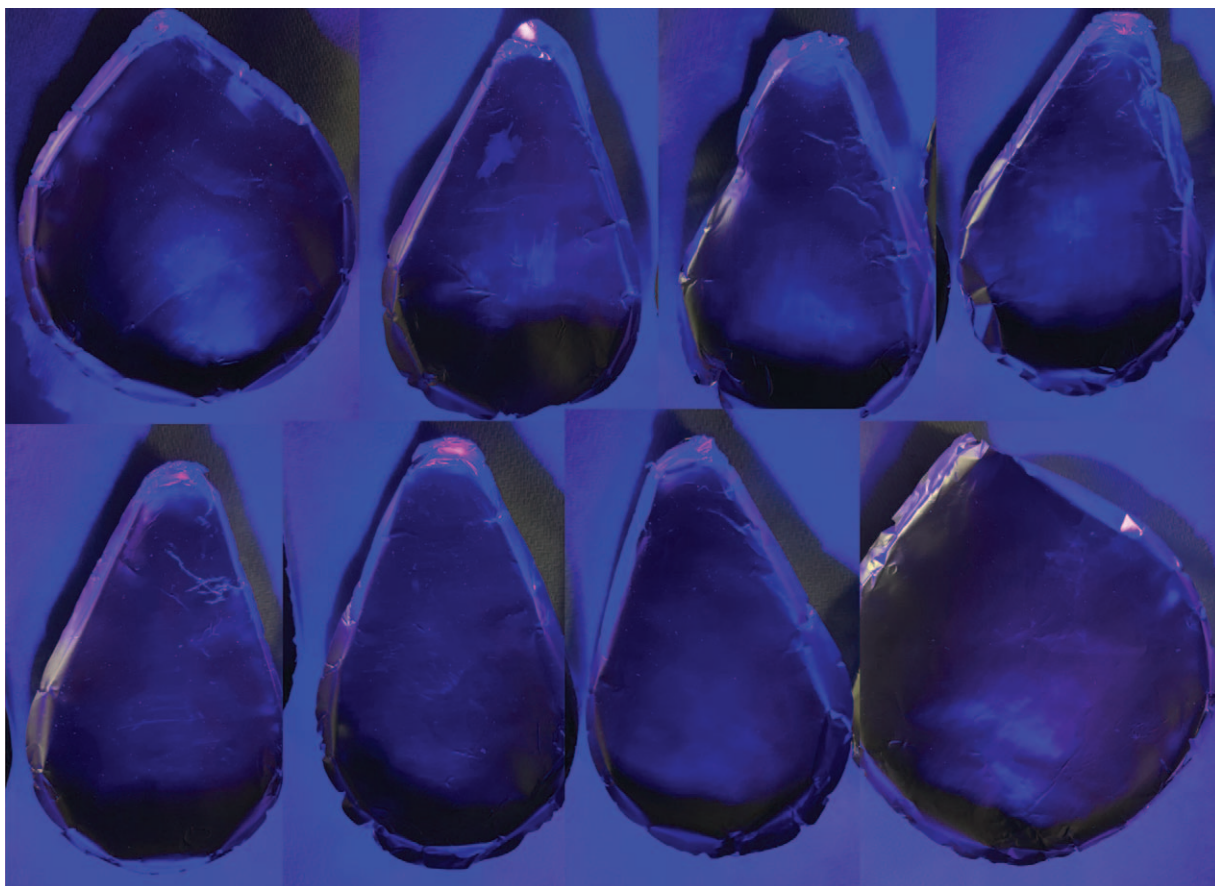


**FIG. 3.** Representative negative impactor trial result. All eight filters were negative in this trial, indicated by no patterns visualized in any filter regardless of room or UV light. This was the trial in which a microscope drape covered the field. Full impactor results are summarized in Table 1.

aerosols (Fig. 3). (Supplemental Video, <http://links.lww.com/MAO/B144>). Table 1 summarizes the impactor results. Photos demonstrating the result of every impactor trial are compiled in supplemental Figures 1 and 2, <http://links.lww.com/MAO/B145>; <http://links.lww.com/MAO/B146>. Supplemental video 1 (<http://links.lww.com/MAO/B144>) demonstrates the experimental set up and footage from several trials.

#### Field Contamination Survey

Drilling of the fluorescent temporal bone model demonstrated several patterns of bone dust and debris scatter. Figure 4 demonstrates the field contamination pattern and density. All scenarios resulted in debris and dust scatter to the tarp edge or beyond the surgical field. Using a 6 cutting bur with no irrigation or suction resulted in heavy distribution of bone dust on the field, the microscope, the surgeon's gown and gloves. There was a plume of fine debris and dust billowing toward the microscope and with the UV light, suspended particles were seen hanging in the air even beyond the tarp (Supplemental Video, <http://links.lww.com/MAO/B144>). The 4 diamond bur without irrigation or suction produced finer particles; there were fewer large particle debris on the tarp with this scenario. Again, there was a plume of bone dust streaming up toward the microscope and

particles visibly suspended in the air beyond the tarp. With the 6 cutting bur using a size 8 handheld suction with the suction aperture continuously occluded, there was still a plume of debris visualized. The use of an additional suction parked adjacent to the specimen did not eliminate the aerosol plumes as there was still suspended debris visualized intermittently. With use of a 6 cutting bur, a handheld suction, and intermittent application of 1 g/L B2 irrigation, there was a plume of debris as well as fluorescent droplets visibly scattered on the tarp, the microscope, and the table beyond the tarp, primarily anteriorly.

General observations during the field contamination trials were that the first part of the mastoidectomy, the removal of the cortex and saucerization, led to the highest volume of bone debris. The 4 diamond bur appeared to create finer bone dust relative to the 6 cutting bur. Increased application of pressure while drilling led to generating more visible debris in the surgical field. As the drilling direction was altered, the location of the generated plume of debris varied. In every trial, there was contamination of the microscope, the surgeon's hands and gloves, and a plume of debris was visualized traveling beyond the tarp. Fine particles visibly suspended in the air were visible with the blacklight. Having the suction in the surgical field did not stop the debris scatter

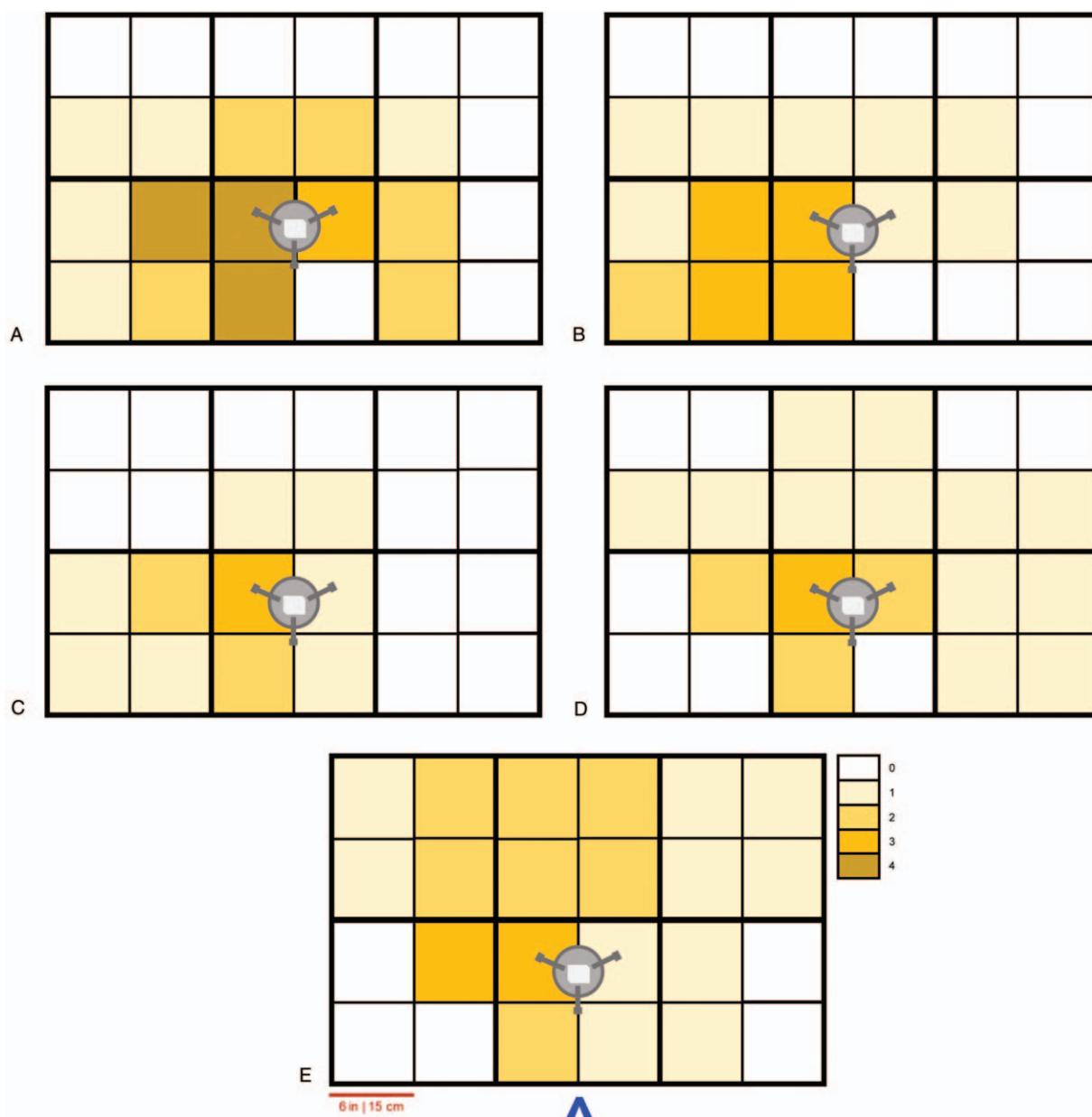


**FIG. 4.** Field contamination studies of simulated mastoidectomy in 3D-printed temporal bone model. *A*, 6 cutting bur, no irrigation, no suction. *B*, 4 diamond bur, no irrigation, no suction. *C*, 6 cutting bur, no irrigation, 1 size 8 handheld suction. *D*, 6 cutting bur, no irrigation, 1 size 8 handheld suction and 1 parked field suction. *E*, 6 cutting bur, vitamin B2 irrigation, 1 size 8 handheld suction. Blue arrow indicates position and direction of right-handed surgeon. Scale: 1 = no particulate matter, 2 = 1–25% coverage, 3 = 25–50% coverage, 4 = major coverage of 50–75%, 5 = 75–100% coverage with layer of caking and excess.

into the air, onto the microscope, the surgeon, or beyond the tarp. Figure 4 demonstrates the density of debris noted on the tarp at the end of each trial.

### DISCUSSION

Understanding aerosol production during mastoid surgery and ways to decrease aerosol production may lead to safer surgery and reduce risk of transmission of SARS-CoV-2 coronavirus. Droplets greater than 20  $\mu\text{m}$  typically fall quickly due to gravity and are usually

too large to be picked up by inhalation streams (13). Particles between 10 and 20  $\mu\text{m}$  may sink to the ground or remain suspended in air. Those that are 10  $\mu\text{m}$  or smaller can be airborne for hours and may travel short or long distances. In one study, the median aerosolized half-life of SARS-CoV-2 was 1 to 1.2 hours, present up to of 3 hours (12), and in another study, viral SARS-Cov-2 RNA was detected in the air from the adjacent hallway (14). Aerosolized particles <5  $\mu\text{m}$  can penetrate deeply into the lower airways and may contribute to an increased likelihood or severity of infection. This study evaluates

aerosol dispersion during a mastoidectomy by assessing the aerodynamic diameter of generated fine particles under 20  $\mu\text{m}$ .

When the cadaveric bone was drilled using the riboflavin (B2) fluorescent irrigation, all eight stages in the impactor contained particulate (Supplemental Figure 2, <http://links.lww.com/MAO/B146>), indicating significant aerosol production under 14.1  $\mu\text{m}$ . This remained the case even when a patent suction was placed immediately adjacent to the specimen during drilling. Suctions have recently been shown to be helpful in endonasal surgery to reduce aerosol risk (15,16); however based on our data, a single standard suction plus a handheld 8 French suction did not make a noticeable impact, as evidenced by the field contamination survey and diffusely positive impactor results (stages 1–8 for cadaveric bone, stages 1–6 for 3D-printed bone). It is possible that with a stronger suction or larger bore suction tubing could make a difference and further testing could elucidate this. Although parking a large suction by the field during mastoidectomy did not eliminate aerosol detection in this study, given the benefit of a parked suction previously demonstrated for endonasal surgery (15) which is more of a closed system, we think in parking a large suction under the drape, which may help to evacuate aerosol particles at risk for escaping during drape manipulation (such as during removal of hands during instrument exchange). Adding a suction under the drape was recently supported by Chari et al. (5).

This study demonstrates that aerosols of sizes known to enter the airways (17) are generated during mastoidectomy. As the middle ear and mastoid mucosa are in continuity with the nasopharyngeal mucosa, we would argue for taking caution during mastoid drilling. Because this was a cadaveric study and not in patients with COVID-19, we were not able to test for the presence of viral particles nor comment on the infectivity of aerosols and droplets generated during mastoidectomy. The infectious potential of bioaerosols generated during many procedures is still unclear. One study using an impactor and hemoglobin testing demonstrated the presence of blood in respirable sized aerosols generated with using common surgical power tools, including a Stryker bone saw, Hall drill, Shea drill, and Bovie electrocautery (18,19). Other studies similarly noted evidence of blood in aerosols when performing powered dental procedures (20–22). Hilal et al. (23) demonstrated that red food dye representing blood scattered as far as 50 cm toward the operator when the drill was at 25,000 RPM, and that fish cornea placed at the surgeon's distance were filled with bone particles after mastoidectomy. Scott et al. (24) demonstrated evidence of neural tissue in bone dust generated during mastoidectomy, raising the question of prion transmission. Despite demonstration of aerosol and debris generated by drilling, the risk of disease transmission is unclear and may vary for bloodborne and viral respiratory illnesses. Further work on infectivity of agents aerosolized during surgery is needed.

Until infectivity has been demonstrated otherwise, it is important to focus on aerosol mitigation to minimize the potential transmission risk of SARS-CoV-2 virus.

The 3D-printed results from this study corroborate with the cadaveric results. Drilling created significant aerosolization of material despite modifying variables such as drill size, suction, and irrigation. A parked suction did not eliminate the detected aerosol for either group. The only mitigation factor that led to negative detection of fine aerosols was using an additional microscope drape as a barrier while drilling. Chen et al. in their study used image analysis to evaluate field contamination and found that placing a 1,060 sterile drape was successful at limiting particulate matter dispersion; however, the authors did not survey fine aerosols below 20  $\mu\text{m}$ .<sup>3</sup> Our results support that fine aerosol dispersion is eliminated with use of an additional barrier drape. The drape trial had completely negative results in stages 1 to 8, indicating aerosols under 14.1  $\mu\text{m}$  were no longer detected. Using an additional drape to cover the surgical field is a successful mitigation measure to reduce aerosol exposure during mastoidectomy.

Using an additional microscope drape to cover the field does require an adjustment from regular practice, but ultimately given that mastoid surgery is performed under a microscope, this does not result in limited visualization or performance in our experience. At our institution, we have begun to use two microscope drapes with each drilling case. The first drape is applied in standard fashion over the microscope. The microscope lens portion is removed from the second drape, leaving a small hole that is then fit around the lens piece of the first drape and secured with tape. The second drape is then flipped inside out to cover the field. The surgeon must lift the drape whenever he or she is exchanging instruments. The eyepiece extensions of the drape may be used as an access port for the surgeon's arms, or may be left untouched. Figure 5 shows the microscope drape in use during a recent surgery.

There are several limitations to this study. Aerosol and debris dispersion data from 3D-printed models and cadaveric specimens may not be directly extrapolated to real surgical scenarios as the temporal bone particles may have a different dispersion pattern *in vivo*. The fluorescent irrigation was used as a surrogate marker for the cadaveric bone mastoid fluid and mucosa; it is unclear whether using a direct fluorescent mucosal marker may have yielded a different dispersion pattern. Although the cascade impactor is a highly reliable instrument for evaluating aerosol dispersion, larger particles with aerodynamic diameters  $>14.1 \mu\text{m}$  were not collected in the simulations. Since simulation scenarios were not replicated multiple times, definitive comparisons between scenarios may be difficult to establish. Visual inspection was used for field coverage estimation and for impactor filter scoring, so particles too small or too few to see may be underreported.

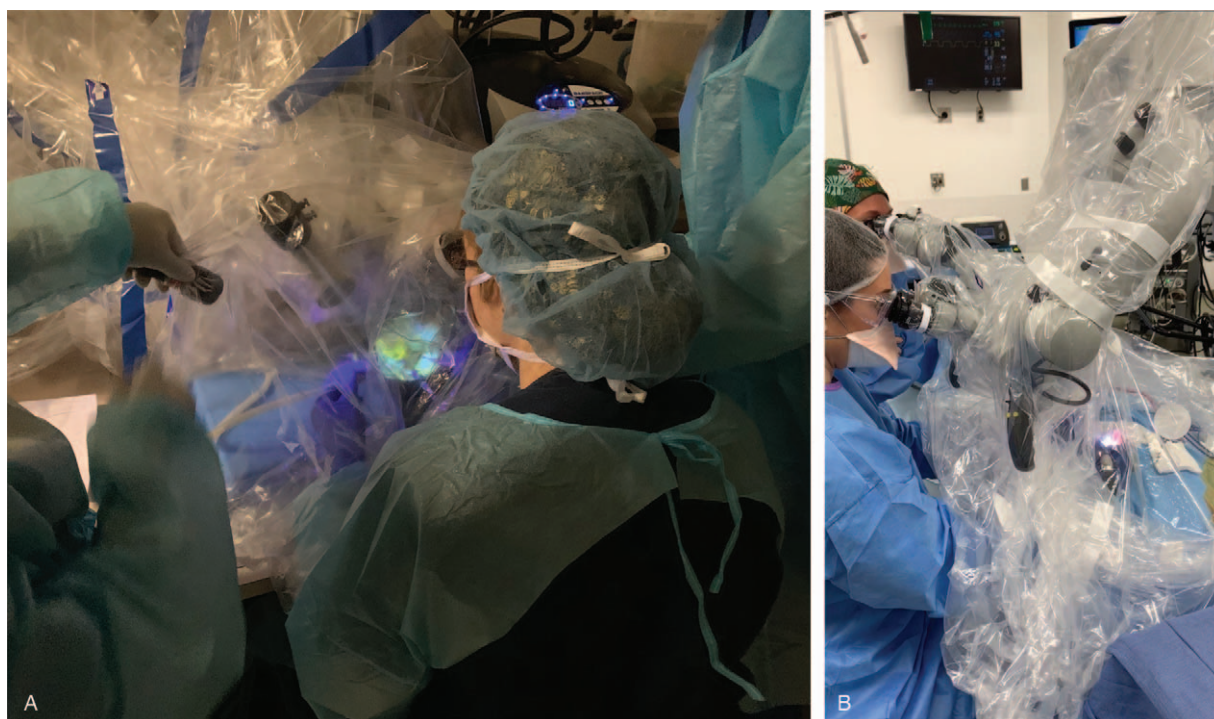


**FIG. 5.** Microscope draping method. **A**, Experimental draping trial with the cadaveric temporal bone and B2 irrigation under UV light. **B**, Example of draping used in the operating room. A second microscope drape with the lens cover removed is secured around the existing drape's lens cover with tape and flipped inside-out to cover the field.

This study does not quantify the volume or mass of aerosol generated, which likely can vary based on multiple factors such as the surgeon's technique and pressure, the quantity and density of the drilled bone, the time spent drilling, suction strength, the distance of the sampling port from the field, and irrigation style. This study was designed to detect dramatic changes in aerosol detection and thus discover strong mitigation factors, but more subtle reductions or increases that may be present from surgeon factors, patient factors and manipulations such as adding a parked suction or increasing irrigation are not quantifiable (such as on a dose–response curve) with this study. Suction and irrigation were not found to be strong mitigation factors in this study, but having a drape was a strong mitigation factor, leading to elimination of detected aerosol at all eight stages. Although the field contamination results demonstrated here represent a specific combination of variables that may not be equivalent for every live case, the potential for significant debris scatter, including debris that was suspended in the air and floating off the field, is demonstrated in this study and supports the need for mitigation factors when performing mastoidectomy.

This study not only has implications for mastoid surgery, but also for any surgery in which drilling is performed in an open field, such as with external approaches to the skull. Given the diffusely positive generation of aerosols during open drilling of bone, strategies for surgeries not amenable to drape use are

needed to mitigate aerosol spread during open drilling for those cases.

## CONCLUSIONS

Fine aerosols are generated with drilling the mastoid. Using an additional microscope drape to cover the surgical field was an effective mitigation strategy to prevent fine aerosol dispersion while drilling.

**Acknowledgments:** Thank you to the Children's Hospital of Pittsburgh resident (Dr. Lindsey Goyal, M.D.), fellow (Dr. Rachel Whelan, M.D.), faculty, and operating room staff who assisted with the mastoidectomy drape demonstration.

## REFERENCES

1. Givi B, Schiff BA, Chinn SB, et al. Safety recommendations for evaluation and surgery of the head and neck during the COVID-19 pandemic. *JAMA Otolaryngol Head Neck Surg* 2020;146:579.
2. Thamboo A, Lea J, Sommer DD, et al. Clinical evidence based review and recommendations of aerosol generating medical procedures in otolaryngology – head and neck surgery during the COVID-19 pandemic. *J Otolaryngol Head Neck Surg* 2020;49:.. article no. 28.
3. Chen J, Workman A, Chari D, et al. Demonstration and mitigation of aerosol and particle dispersion during mastoidectomy relevant to the Covid-19 Era. *Otol Neurotol* 2020. Online ahead of print.
4. Sharma D, Rubel K, Ye M, et al. Cadaveric simulation of otologic procedures: An analysis of droplet splatter patterns during the COVID-19 Pandemic. *Otolaryngol Head Neck Surg* 2020;163:320–4.

5. Chari DA, Workman AD, Chen JX, et al. Aerosol dispersion during mastoidectomy and custom mitigation strategies for otologic surgery in the COVID-19 Era. *Otolaryngol Head Neck Surg* 2020. 0194599820941835.
6. Norris BK, Goodier AP, Eby TL. Assessment of air quality during mastoidectomy. *Otolaryngol Head Neck Surg* 2011;144:408–11.
7. Tellier R, Li Y, Cowling BJ, Tang JW. Recognition of aerosol transmission of infectious agents: A commentary. *BMC Infect Dis* 2019;19: article 101.
8. Marple VA, Olson BA, Santhanakrishnan K, Roberts DL, Mitchell JP, Hudson-Curtis BL. Next generation pharmaceutical impactor: A new impactor for pharmaceutical inhaler testing. Part III. extension of archival calibration to 15 L/min. *J Aerosol Med* 2004;17:335–43.
9. Yang H, Xiao X, Zhao X, et al. Study on fluorescence spectra of thiamine and riboflavin. *MATEC Web of Conferences* 2016;63:03013.
10. Sim ES, Dharmarajan H, Boorgu DSSK, et al. Novel use of vitamin B2 as a fluorescent tracer in aerosol and droplet contamination models in otolaryngology. *Ann Otol Rhinol Laryngol* 2020;000 3489420949588.
11. Freiser ME, Ghodadra A, Hirsch BE, McCall AA. Evaluation of 3D printed temporal bone models in preparation for middle cranial fossa surgery. *Otol Neurotol* 2019;40:246–53.
12. van Doremalen N, Bushmaker T, Morris DH, et al. Aerosol and surface stability of SARS-CoV-2 as compared with SARS-Cov-1. *N Engl J Med* 2020;382:1564–7.
13. Anderson EL, Turnham P, Griffin JR, Clarke CC. Consideration of the aerosol transmission for COVID-10 and public health. *Risk Anal* 2020;40:902–7.
14. Guo Z-D, Wang Z-Y, Zhang S-F, et al. Aerosol and surface distribution of severe acute respiratory syndrome Coronavirus 2 in Hospital Wards, Wuhan, China, 2020. *Emerg Infect Dis* 2020;26:1583–91.
15. Dharmarajan H, Freiser ME, Sim E, et al. Droplet and aerosol generation with endonasal surgery: Methods to mitigate risk during the Covi-19 Pandemic. *Otol Head Neck Surg* 2020. 1945998 20949802.
16. Workman AD, Xiao R, Feng A, et al. Suction mitigation of airborne particulate generated during sinonasal drilling and cautery. *Int Forum Allergy Rhinol* 2020. [Epub ahead of print].
17. Baron P. Generation and Behavior of Airborne Particles (Aerosols). Centers for Disease Control and Prevention. Available at: [https://www.cdc.gov/niosh/topics/aerosols/pdfs/Aerosol\\_101.pdf](https://www.cdc.gov/niosh/topics/aerosols/pdfs/Aerosol_101.pdf). Accessed June 6, 2020.
18. Jewett DL, Heinsohn P, Bennett C, Rosen A, Neuilly C. Blood-containing aerosols generated by surgical techniques: A possible infectious hazard. *Am Ind Hyg Assoc J* 1992;53: 228–31.
19. Perdelli F, Spagnolo A, Cristina M, et al. Evaluation of contamination by blood aerosols produced during various healthcare procedures. *J Hosp Infect* 2008;70:174–9.
20. Cristina M, Spagnolo A, Sartini M, et al. Evaluation of the risk of infection through exposure to aerosols and spatters in dentistry. *Am J Infect Control* 2008;36:304–7.
21. Szymanska J. Dental bioaerosol as an occupational hazard in a dentist's workplace. *Ann Agric Environ Med* 2007;14:203–7.
22. Miller RL. Characteristics of blood-containing aerosols generated by common powered dental instruments. *Am Ind Hyg Assoc J* 1995;56:670–6.
23. Hilal A, Walshe P, Gendy S, Knowles S, Burns H. Mastoidectomy and trans-corneal viral transmission. *Laryngoscope* 2005;115: 1873–6.
24. Scott A, De R, Sadek SAA, Garrido MC, Path MRC, Courteney-Harris RG. Temporal bone dissection: A possible route for prion transmission? *J Laryngol Otol* 2001;115:374–5.